A mechanical microscope: High-speed atomic force microscopy

A. D. L. Humphris,[a] M. J. Miles, and J. K. Hobbs[b]
University of Bristol, H.H. Wills Physics Laboratory, Tyndall Avenue, Bristol, BS8 1TL, United Kingdom

(Received 4 August 2004; accepted 14 December 2004; published online 14 January 2005)

An atomic force microscope capable of obtaining images in less than 20 ms is presented. By utilizing a microresonator as a scan stage, and through the implementation of a passive mechanical feedback loop with a bandwidth of more than 2 MHz, a 1000-fold increase in image acquisition rate relative to a conventional atomic force microscope is obtained. This has allowed images of soft crystalline and molten polymer surfaces to be collected in 14.3 ms, with a tip velocity of 22.4 cm s^{-1} while maintaining nanometer resolution. © *2005 American Institute of Physics*.
[DOI: 10.1063/1.1855407]

Since its invention in 1986[1] atomic force microscopy (AFM) has become the most widely used form of scanning probe microscope (SPM) with applications in surface, materials, and biological sciences.[2,3] However, the inherent mechanical nature of the AFM, requiring the serial collection of the image, limits the microscope's maximum speed of operation. A typical image is collected over a period of ~30 s, which is much slower than the millisecond time resolution required for the visualization of macromolecular process, and restricts nonimaging applications such as nanolithography[4,5] and data storage.[6]

Integral to the AFM is a sharp stylus, which is mounted on the end of a microcantilever. By raster scanning the stylus across the surface of the sample and monitoring the deflection of the microcantilever beam an interaction map and thus image is constructed. The image acquisition time of an AFM, and in fact any SPM, is limited by three factors: (i) the measurement bandwidth of the local interaction between the tip and sample, (ii) the rate at which the tip can scan the surface of the sample in an *x*, *y* plane, and (iii) how quickly the tip can follow the contours of the sample. Recently these limits have been addressed by miniaturizing the microcantilever and constructing small, lower mass and high stiffness scanners. This has achieved image acquisition rates of ~12 frames/s[7] but is limited to imaging small areas of $\sim 250 \times 250$ nm with a maximum tip velocity of ~600 μm/s.[8] An alternative approach has been to incorporate a piezo actuator into the AFM cantilever, increasing the frequency response of the feedback loop enabling a maximum tip velocity of 5 mm s^{-1}.[9] Ultimately this approach of refining instrument design will reach a limit that is arguably not far from the capabilities already demonstrated.

This letter introduces a physically different implementation of an AFM that is not limited by the same constraints as the conventional approach, by solving two fundamental barriers. First, a micro-resonant scanner that has been previously demonstrated by Humphris *et al.*[10] is used to raster the sample relative to the tip. The scanner uses rather than avoids mechanical resonances that limit a conventional scanner. Second, a mechanical feedback loop that is intrinsic to the microcantilever beam, instead of an electronic feedback loop, is used to control the tip–sample interaction and follow contours in the surface of the sample. As shown in the schematic in Fig. 1, the sample is scanned in the *x*, *y* plane beneath the tip of the microcantilever using a micro-resonant scanner constructed from a quartz crystal tuning-fork, to generate the fast scan axis, and piezo actuator, to generate the slow scan axis. In a conventional AFM an electronic feedback loop is used to follow the topography of the sample by adjusting the position of the sample relative to the tip to maintain a constant deflection of the cantilever and thus interaction force. In the high-speed (HSAFM) AFM a passive feedback system is used. A constant external force is applied directly to the tip so as to accelerate the tip toward the sample surface, and the mechanical properties of the microcantilever beam are constructed to control the path of the tip over the surface of the sample. The direct force applied to the tip is independent of the deflection of the microcantilever and is of sufficient magnitude to hold the tip in contact with the surface. Thus the beam of the microcantilever controls the position of the tip in the x–y plane and the trajectory of the tip in the direction perpendicular to the surface of the sample (i.e., the *z* axis), but does not provide a significant bending-dependent force to the surface.

The tip and end of the microcantilever beam is forced to respond to corrugations in the surface of the sample at frequencies far greater than its fundamental mode of bending.

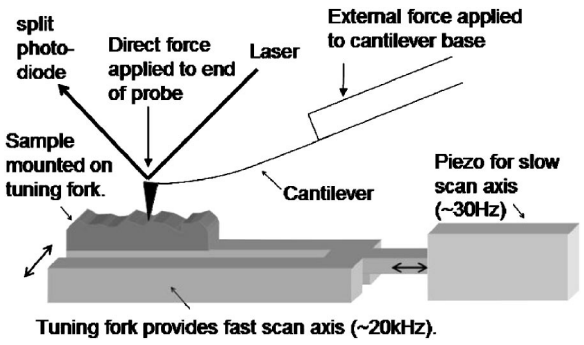

FIG. 1. A schematic of the HSAFM. The sample is mounted on a quartz crystal resonator that generates the fast scan axis and is driven in the orthogonal slow scan axis by a piezo actuator. An optical lever is used to measure the deflection of the microcantilever. An additional "direct force" is applied to the end of the cantilever, forcing the tip to maintain contact with the surface. By tuning the magnitude of the "direct force" and the degree of damping of the cantilever, a high bandwidth passive feedback loop is created.

[a]Author to whom correspondence should be addressed; electronic mail: andy.humphris@bristol.ac.uk
[b]Present address: Department of Chemistry, University of Sheffield, Sheffield, S3 7HF, United Kingdom.

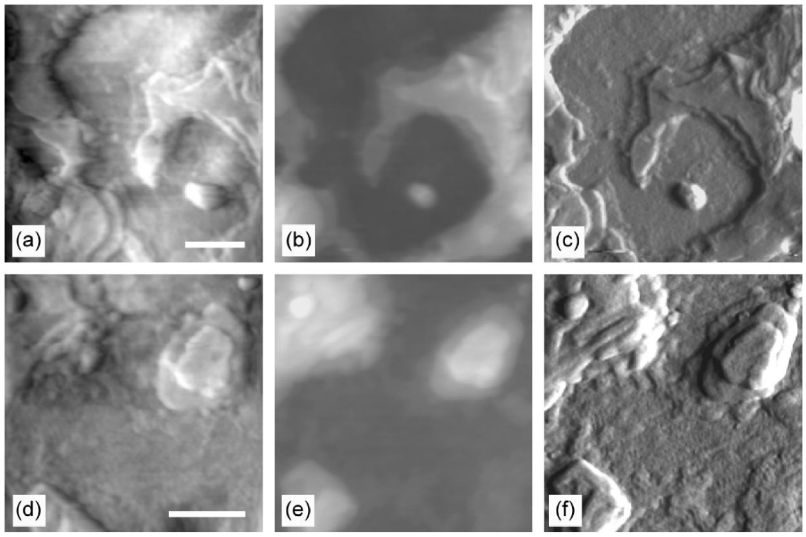

FIG. 2. The images show the surface of crystallized poly(ethylene-oxide) (PEO) on a glass substrate collected using both conventional AFM and HSAFM. (a) and (d) were collected using HSAFM over a period of 14.3 and 15.8 ms with a tip velocity in the centre of the image of 22.4 and 16.8 cm/s, respectively (128 $\times$128 pixels). (b) and (c) show the same area of the sample as image (a) and were collected using conventional AFM displaying the height and deflection of the cantilever (error signal), respectively. (e) and (f) show the same area of the sample as image (d) and were collected using conventional AFM displaying the height and deflection of the cantilever (error signal), respectively. The surface of the soft polymer sample showed no degradation after repeated imaging using both conventional and high speed AFM. Scales bars are 1 μm. Black to white in (b) represents 200 nm, and in (c) represents 180 nm. The information in the HSAFM images are a combination of topographic height and slope information, so the *z* scale does not have a defined unit or calibration.

Impulses supplied to the microcantilever beam via the surface of the sample excite high modes of bending that must be suppressed and any energy removed so that the history of the probes motion does not affect its new trajectory. This is achieved by coating the back of the microcantilever with a thin polymer layer that removes energy, suppressing any motion of the beam. Various mechanisms can be used to generate the deflection independent direct force supplied to the tip. Here a combination of two direct forces was used. First, when working in an ambient environment a capillary water neck forms between the tip and the sample and supplies an attractive force between the tip and the surface, typically of the order of a few nano-newtons. This gives an essentially constant direct force applied to the tip. As it is not easy to control, an additional electrostatic force was applied by introducing a voltage between the conducting coating on the AFM cantilever and a ground plate below the sample surface. Combined, these two forces were sufficient to provide the desired bandwidth.

The HSAFM was constructed within a commercial Veeco Dimension 3100 AFM with Nanoscope IV controller, using the microscope's imaging capabilities to obtain the conventional AFM images, and the existing optical reflection-detection setup for detecting the cantilever bending when operating in high speed mode. Silicon nitride microcantilevers coated in a thin polymer film were used for all experiments. The sample was mounted on the micro-resonant scanner constructed from a quartz crystal tuning fork with the oscillation axis perpendicular to the motion of a 5 μm piezo stack (P-802 and E-505, Physik Instrument, Germany). Dedicated hardware constructed from 100 MHz 12 bit resolution analogue to digital converters and a field programmable gate array was used to capture and simultaneously correct for the sinusoidal velocity of the scanner resulting from the use of resonance, producing a real-time image.

To quantify the lateral and vertical resolution of the HSAFM the surface of crystallized poly(ethylene-oxide) (PEO) was imaged as a test sample. The sample was prepared by solution casting PEO (molecular weight 18 000 Da) from chloroform onto 800 μm glass cubes at 80 °C and then quenching to room temperature. The resulting surface consists of polyethylene oxide lamellae primarily oriented parallel to the substrate. Figures 2(a) and 2(d) show HSAFM images of two different areas of the same sample, each image collected in 14.3 ms. Figures 2(b) and 2(e) show the corresponding conventional mode height images, while Figs. 2(c) and 2(f) show the deflection (or error signal) images collected at the same time as the height images, each image collected in 64 s. The quality of the HSAFM images is comparable to those collected more than 4000 times slower, with vertical resolution better than 1 nm and lateral resolution of approximately 30 nm. By considering the trajectory of the probe when leaving the surface the bandwidth of the mechanical feedback loop has been estimated to be greater than 2 MHz. It has been found that the resolution obtainable with the HSAFM is the same as that obtained when imaging slowly in a conventional "contact mode" of imaging. This resolution is limited by the shape of the imaging tip, and is typically around 10 nm.

To determine the microscope's ability to image soft materials, a thin film of polyhydroxybutyrate-co-valerate (PHB/V) was prepared by melt casting at 180 °C and then quenching to room temperature. The resultant supercooled liquid crystallizes slowly at room temperature to form spherulites. Figure 3 shows a series of images of the growth front of a spherulite during crystallization from the melt, the lower (smooth) portion of each image being molten polymer. This demonstrates that these delicate surfaces can be stably

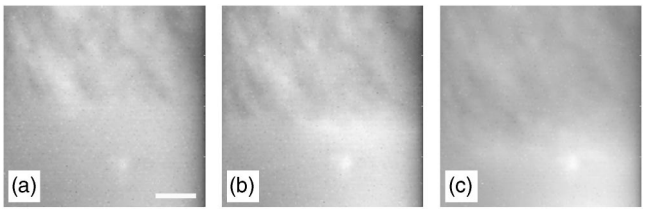

FIG. 3. A series of HSAFM images of the growth front of a polyhydroxybutyrate-co-valerate spherulite crystallizing from the melt. The smooth lower portion of each image is molten polymer. A piece of dirt embedded in the melt can be seen in the lower right of each image. Each 256$\times$256 pixel image was collected in 31 ms. The conventional AFM is not able to stably image the surface of the molten polymer when operating in contact mode. The surface of the crystal is topographically very smooth, with a total height contrast of approximately 10 nm and no sharp variations, hence the relatively low image contrast in these images. The contrast in the final image was reduced relative to the previous two images as the piece of dirt referred to earlier is being pushed up by the motion of the melt as the growth front approaches, requiring the vertical scale to be extended. The scale bar represents 500 nm.

imaged using the HSAFM, which is not possible with a conventional AFM using a contact mode of operation. The principle difference when using the HSAFM is that the tip velocity is higher by approximately 1000 times. This means that, for a 10 nm radius tip, any region of the sample is in contact with the tip for less than 1 μs during each scan-line, compared to 1 ms for a conventional AFM. If an energy barrier has to be overcome to damage the surface, the probability of crossing that barrier will depend on the length of time over which a force is applied. So, reducing the tip–sample interaction time will reduce the probability of damaging the surface. Thus the HSAFM not only gives reduced image acquisition times but also minimizes sample disturbance by the tip.

Finally, it was found that the high image rates obtained with the HSAFM give considerable improvement in the microscope's stability. High image rates will always improve stability, as low frequency noise ($<$10 Hz) will cause motion of entire images, rather than disturbance of individual lines, while the necessary high bandwidth of the "feedback loop" maintains contact between the probe and the surface. Additionally, in the case of the HSAFM, by using a resonator with a high quality factor as the micro-scanner, image stability is further improved as any external impulse (noise) naturally decays over many cycles of the resonance.

In summary, by utilizing a micro-resonant scanner and mechanical feedback loop, an AFM capable of 70 frames/s has been demonstrated, each image collected in less than 15 ms. This is over 1000 times faster than a conventional AFM and over 5 times faster than the maximum rate achieved by other nonconventional approaches to AFM.[6]

The authors acknowledge the assistance of K. P. Mandelin and D. J. Catto (Infinitesima Ltd., UK) with electronic and software aspects of this work. J.K.H. would like to thank the Engineering and Physical Science Council, UK and A.D.L.H. the Royal Commission for the Exhibition of 1851.

[1] G. Binnig, C. F. Quate, and Ch. Gerber, Phys. Rev. Lett. **56**, 930 (1986).
[2] J. K. H. Horber and M. J. Miles, Science **302**, 1002 (2003).
[3] F. Oesterhelt, D. Oesterhelt, M. Pfeiffer, A. Engel, H. E. Gaub, and D. J. Muller, Science **288**, 143 (2000).
[4] S. Snow and P. M. Campbell, Science **270**, 1639 (1995).
[5] R. D. Piner, J. Zhu, F. Xu, S. Hong, and C. A. Mirkin, Science **283**, 661 (1999).
[6] P. Vettiger, G. Cross, M. Despont, U. Drechsler, U. Durig, B. Gotsmann, W. Haberle, M. A. Lantz, H. E. Rothuizen, R. Stutz, and G. K. Binnig, IEEE Trans. Nanotechnol. **1**, 39 (2002).
[7] D. A. Walters, J. P. Cleveland, N. H. Thomson, P. K. Hansma, M. A. Wendman, G. Gurley, and V. Elings, Rev. Sci. Instrum. **67**, 3583 (1996).
[8] T. Ando, N. Kodera, E. Takai, D. Maruyama, K. Saito, and A. Toda, Proc. Natl. Acad. Sci. U.S.A. **98**, 12468 (2001).
[9] T. Sulchek, R. Hsieh, J. D. Adams, S. C. Minne, C. F. Quate, and D. M. Adderton, Rev. Sci. Instrum. **71**, 2097 (2000).
[10] A. D. L. Humphris, J. K. Hobbs, and M. J. Miles, Appl. Phys. Lett. **83**, 6 (2003).